Author Manuscript

Author Manuscript

Author Manuscript

Author Manuscript

HHS Public Access

Author manuscript

Nature. Author manuscript; available in PMC 2012 November 16.

Published in final edited form as:

Nature. ; 485(7398): 395–399. doi:10.1038/nature11085.

Structure of the Nociceptin/Orphanin FQ Receptor in Complex with a Peptide Mimetic

Aaron A. Thompson[1,§], **Wei Liu**[1,§], **Eugene Chun**[1,§], **Vsevolod Katritch**[1], **Huixian Wu**[1], **Eyal Vardy**[2], **Xi-Ping Huang**[2], **Claudio Trapella**[3], **Remo Guerrini**[3], **Girolamo Calo**[4], **Bryan L. Roth**[2], **Vadim Cherezov**[1], and **Raymond C. Stevens**[1,*]

[1]Department of Molecular Biology, The Scripps Research Institute, La Jolla, CA 92037, USA

[2]National Institute of Mental Health Psychoactive Drug Screening Program, Department of Pharmacology and Division of Chemical Biology and Medicinal Chemistry, University of North Carolina Chapel Hill Medical School, Chapel Hill, NC 27599, USA

[3]Department of Pharmaceutical Sciences and LTTA (Laboratorio per le Tecnologie delle Terapie Avanzate), University of Ferrara, 44121 Ferrara, Italy

[4]Department of Experimental and Clinical Medicine, Section of Pharmacology and National Institute of Neuroscience, University of Ferrara, 44121 Ferrara, Italy

Abstract

Members of the Opioid Receptor (OR) family of G protein-coupled receptors (GPCRs) are found throughout the peripheral and central nervous system where they play key roles in nociception and analgesia. Unlike the classical ORs, δ–OR, κ–OR,[1] and μ-OR,[2] which were delineated by pharmacological criteria in the 1970's and 1980's, the nociceptin/orphanin FQ (N/OFQ) peptide receptor (NOP, aka ORL-1) was discovered relatively recently via molecular cloning and characterization of an orphan GPCR[3]. Despite its high sequence similarity (~60%) with ORs, NOP has a strikingly distinct pharmacology[4,5]. Despite high sequence similarity with classical opioid G protein-coupled receptor subtypes, the nociceptin/orphanin FQ (N/OFQ) peptide receptor (NOP)

Users may view, print, copy, download and text and data- mine the content in such documents, for the purposes of academic research, subject always to the full Conditions of use: http://www.nature.com/authors/editorial_policies/license.html#terms

*Address correspondence to: The Scripps Research Institute, 10550 North Torrey Pines Rd., GAC-1200, La Jolla, CA 92037. Tel.: 858-784-9416; Fax: 858-784-9483; stevens@scripps.edu.

§These authors contributed equally to this work

Supplementary Information is linked to the online version of the paper at (web).

Author Contributions A.T. optimized the constructs, purified and crystallized the receptor in LCP, optimized crystallization conditions, grew crystals for data collection, collected the data and refined the structure, and prepared the manuscript. W.L. assisted with LCP experiments, performed FRAP, collected diffraction data, and assisted with preparing the manuscript. E.C. assisted in construct optimization, assisted with LCP experiments, collected diffraction data, and assisted with preparing the manuscript. V.K. performed the receptor docking and prepared the manuscript. H.W. assisted with membrane preparations, provided advice on crystallization strategies, and assisted with preparing the manuscript. E.V. and X.-P.H. performed ligand-binding and site-directed mutagenesis studies. C.T., R.G. and G.C. suggested the use of and synthesized numerous ligands for crystallization and pharmacological studies, and assisted with preparing the manuscript. B.L.R. supervised the pharmacology and mutagenesis studies and prepared the manuscript. V.C. assisted with the crystallization in LCP, collected diffraction data, processed diffraction data, and prepared the manuscript. R.C.S. was responsible for the overall project strategy and management and wrote the manuscript.

Author Information The coordinates and the structure factors have been deposited in the Protein Data Bank under the accession code (4EA3). Reprints and permissions information is available at (web). R.C.S. is a founder and Board of Directors member of Receptos, a GPCR drug discovery company. Readers are welcome to comment on the online version of this article at (web).

Author Manuscript Author Manuscript Author Manuscript Author Manuscript

has a distinct biological and pharmacological role, featuring activation by the endogenous peptide N/OFQ, and unique selectivity for exogenous ligands. This study reports the crystal structure of human NOP solved in complex with the peptide mimetic antagonist Banyu Compound-24 (C-24), revealing atomic details of ligand-receptor recognition and selectivity. C-24 mimics the first four N-terminal residues of the NOP-selective peptide antagonist UFP-101, a close derivative of N/OFQ, and provides important clues to binding of these peptides. The X-ray structure also reveals substantial conformational differences in the pocket regions between NOP and the "classical" opioid receptors κ (Ref. 1) and μ (Ref. 2), which are likely due to a small number of residues that vary between the two receptors. The NOP/C-24 structure explains the divergent selectivity profile of NOP and provides a new structural template for the design of NOP ligands.

The pharmacological effects of N/OFQ are complex and distinct from classical ORs. N/OFQ displays sequence similarity with other opioid peptides, notably the κ–OR endogenous ligand dynorphin A, but does not interact with δ–OR, κ–OR, or μ-OR. Similarly, the classical opioid peptides have very low affinity for NOP. Unlike the classical ORs, NOP is also insensitive to most morphine-like small molecules including naloxone, thereby yielding a pharmacologically important discriminatory feature between NOP and classical ORs. Studies with N/OFQ, NOP selective agonists and antagonists, and receptor or peptide deficient mice have shown that the NOP system has important roles in the control of central and peripheral functions including pain, anxiety and mood, food intake, learning and memory, locomotion, cough and micturition reflexes, cardiovascular homeostasis, intestinal motility, and immune responses[6]. Understanding the structural requirements for NOP ligand selectivity and modes of binding is therefore paramount for the optimization of future agonist and antagonist-based therapeutics.

By replacing the N-terminal residues of the human NOP receptor with thermostabilised apocytochrome b_{562}RIL (BRIL)[7] and truncating 31 C-terminal residues (see Supplementary Methods), we determined the 3.0 Å resolution X-ray crystal structure of this receptor in complex with Compound-24 (C-24), a small peptide mimetic antagonist[8] (Fig. 1a). We found that this BRIL-NOP fusion is functional and responds to N/OFQ and the small molecular agonist SCH-221510[9], activating endogenous $G_{i/o}$ proteins in HEK 293-T cells, albeit with reduced potency and efficacy (Supplementary Tables 2,3), perhaps due to the C-terminal NOP truncation. C-24 was selected for co-crystallization based on the pronounced thermostability it imparts on the receptor (Supplementary Fig. 1), its high affinity (IC_{50} = 0.27 nM) and antagonist potency (IC_{50} = 0.15 nM) for NOP, and selectivity (≥ 1000-fold)[8]. Peripherally administered C-24 is able to penetrate the CNS where it antagonizes N/OFQ effects on nociception[10] and produces beneficial responses in experimental models of Parkinson's disease[11]. The NOP structure revealed C-24 binding deep within the orthosteric binding pocket (Fig. 1a) likely mimicking the "message" domain of N/OFQ (Phe1-Gly2-Gly3-Phe4), a sequence similar to that of canonical opioid peptides (Tyr1-Gly2-Gly3-Phe4)[6,12] (Supplementary Fig. 2). Structural comparison of published GPCR crystal structures reveals a modularity of the 7TM core and significant variation of the extracellular (EC) module with boundaries defined by proline induced kinks[13]. NOP contains five such kinks in the 7TM core located at residue positions Pro105$^{2.58}$, Pro184$^{4.59}$, Pro227$^{5.50}$, Pro278$^{6.50}$, and Pro316$^{7.50}$ (superscripts indicate residue numbers as per the Ballesteros-

Author Manuscript Author Manuscript Author Manuscript Author Manuscript

Weinstein nomenclature[14]), yielding repercussions on the shape of the ligand binding pocket. Importantly, the EC tip of helix V in NOP is shifted by more than 4 Å as compared with the κ–OR[1] and μ-OR[2] crystal structures thereby resulting in both a gap between helices IV and V (~12 Å between C_α of residues 184 and 215) and an expansion of the orthosteric pocket (Supplementary Fig. 5). However, compared with CXCR4, the EC tip of helices VI and VII are tilted *in* towards the orthosteric pocket. Unlike the κ–OR structure[1], the EC half of helix I in NOP is pulled *in* towards the axis of the TM bundle in a conformation that is more similar to that of the chemokine receptor (PDB ID 3ODU[15]; Fig. 1b). This alternate conformation of helix I is facilitated by the presence of flexible glycine residues located at an apparent 'hinge point' that are conserved within the OR family: Gly65$^{1.46}$ and Gly68$^{1.49}$ in NOP, and Gly73$^{1.46}$ and Gly76$^{1.49}$ inκ–OR. NOP has an additional glycine at the 'hinge point', Gly64$^{1.45}$, adding to the potential flexibility of this helix.

Despite low sequence conservation, extracellular loops (ECLs) 1 and 2 of NOP are structurally similar to those of κ–OR and CXCR4 (Fig. 1b). Specifically, the backbone of ECL1 in NOP is nearly indistinguishable from that of κ–OR and CXCR4. ECL2 forms an elongated βhairpin, which is tethered to the EC tip of helix III by a structurally conserved disulfide bond between Cys123$^{3.25}$ and Cys200^{ECL2}. This β-hairpin motif is also observed in κ–OR and CXCR4, suggesting a common structural motif of the γ-branch[16] Class A peptide binding receptors. Unlike δ–OR and μ-OR, the ECL2s of κ–OR and NOP are enriched in aspartate and glutamate residues making the loop and the entrance to their binding pocket very acidic (Supplementary Fig. 6). Moreover, ECL2 in NOP is two residues shorter than in κ–OR, making it and differences in charge distribution possible determinants for selectivity. These details are consistent with N/OFQ / dynorphin A chimera peptide data showing that replacement of as few as six residues on N/OFQ with the corresponding residues from dynorphin A dramatically impaired affinity and activity towards NOP[17].

The intracellular loop (ICL) 2 of NOP receptor 'B' forms a short α-helix, which has been observed in a number of other GPCRs; and ICL3 of NOP receptor 'A' is structured and connects helices V and VI allowing this region to extend into the cytoplasm for interaction with heterotrimeric G_i/G_o proteins (Fig. 1c). Structural alignment with thermostabilized $A_{2A}AR$[18] (PDB ID 3PWH) reveals a similar orientation of helices V and VI, although the helices are shorter in the NOP structure (Fig. 1c, Supplementary Fig. 7). The loop regions of these ICL3s are conformationally dissimilar, and differ in length by seven residues (8 residues long in $A_{2A}AR$ versus 15 residues in NOP). Both ICL2 and ICL3 are tethered to the 7TM core, restricting their mobility, through interactions involving arginine residues that are conserved within the OR family: Arg162^{ICL2} forms a salt bridge with Asp147$^{3.49}$ to the conserved D(E)RY motif, and Arg259$^{6.31}$ forms a hydrogen bond with the backbone carbonyl with Val245^{ICL3} (Supplementary Fig. 7).

The NOP/C-24 structure highlights specific residues in the pocket essential for N/OFQ binding and receptor subtype selectivity (Fig. 2). The orthosteric binding pocket of NOP is relatively large, reflecting its ability to bind large endogenous peptides. With a similar pose in both NOP molecules (RMSD = 0.6 Å), C-24 interacts with the 'floor' of the pocket through several hydrophobic and electrostatic interactions. Mutagenesis of the NOP's binding pocket defined the relative impact of specific residues on C-24 and N/OFQ binding

Author Manuscript Author Manuscript Author Manuscript Author Manuscript

and function (Supplementary Tables 4,5). The protonated nitrogen of the C-24 piperidine ring forms a crucial salt bridge with Asp130$^{3.32}$, a residue that is conserved in the OR family and all biogenic amine GPCRs. Mutations of Asp130$^{3.32}$ to either alanine or asparagine abrogate N/OFQ binding, highlighting the requirement of the negative charge at this position[19] (Fig. 2 and Supplementary Tables 4,5). Numerous studies have proposed that Asp130$^{3.32}$ is involved in a salt bridge interaction with the positively charged N-terminal nitrogen of N/OFQ [20,21]. In addition to the anchoring salt bridge between Asp130$^{3.32}$ and the amino moiety of C-24, the linked benzofuran/piperidine rings are buried in a hydrophobic pocket created by residues from helices III, V and VI. The benzofuran 'head' group is sandwiched between Met134$^{3.36}$ and Tyr131$^{3.33}$, where the Met$^{3.36}$ side chain adopts a different, more buried rotamer as compared to κ–OR, thereby allowing a deeper penetration of the C-24 ring system. This is further emphasized by the modest effect of a Met134$^{3.36}$Ala mutation on the potency of NOP ligands (Supplementary Tables 4,5). A Tyr131$^{3.33}$Phemutation had no effect on agonist binding while Tyr131$^{3.33}$Ala was deleterious (Supplementary Tables 4,5) suggesting that Tyr131 participates in π-stacking interactions with Phe1 of the peptide[19].

At the 'tail' end of C-24, the carbonyl group adjacent to the pyrrolidine ring is hydrogen bonded to Gln107$^{2.60}$, a residue stabilized by a hydrogen bond to Tyr309$^{7.43}$. While a Gln107$^{2.60}$Ala mutation results in a 10-fold loss in C-24 binding and over 300-fold reduction in N/OFQ potency, mutation of Tyr309$^{7.43}$ abolishes binding of C-24 and reduces N/OFQ potency ~7-fold (Supplementary Tables 4–5). Interestingly, both Gln$^{2.60}$ and Tyr$^{7.43}$ are present in the κ–OR structure, albeit in very different conformations (Supplementary Fig. 8).

The crystal structure of NOP in complex with C-24 afforded us a unique opportunity to elucidate the molecular basis for both the high affinity binding by N/OFQ derived peptide antagonists and their pronounced subtype selectivities (Fig. 3). Importantly, we verified that the C-24 binding mode can be reliably reproduced by energy-based docking of C-24 to the NOP receptor with an RMSD ~ 0.9 Å. Moreover, docking of another piperidine derivative, Compound-35 (C-35)[22], closely mimics the binding of C-24, while docking a less active stereoisomer Compound-36[22] yields a significantly distorted binding pose in the pyrrolidine region and a reduced binding score (not shown). Previously, Trapella et al.[22] proposed that C-24 mimics the N-terminal four residues of N/OFQ related peptide antagonists [Nphe1]N/OFQ(1-–3)-NH_2 (ref [23]) and UFP-101 (ref [24]). Automated docking of the four N-terminal residues of UFP-101 results in a conformation of the Nphe1-Gly2-Gly3-Phe4 tetrapeptide where the Nphe1 and Phe4 rings of the peptide make the same hydrophobic interactions as the aromatic rings of C-24, and the N-terminal amino group forms a salt bridge with Asp130$^{3.32}$, thus supporting the proposed similarity in the binding poses between small molecules and peptide analogues (Fig. 3c).

The "address" domain of N/OFQ (residues 5–17) was previously shown by NMR to have a strong preference for α-helical secondary structure[25,26], which is likely preserved in UFP-101 since the only difference in this domain are the mutations Leu14Arg and Ala15Lys. Docking of the full-length UFP-101 suggests a plausible fit of the α-helical address domain into the binding pocket entrance shaped by the highly acidic tip of ECL2

Author Manuscript Author Manuscript Author Manuscript Author Manuscript

and helices II and VII, with all six basic residues of the peptide forming ionic interactions with acidic side chains of NOP (Fig. 3c,d,e).

Interactions of the "address" domain of N/OFQ(1–13) with helices II (residues 107–113)[27] and VII (residues 296–302)[19] were previously demonstrated by photocrosslinking, a finding consistent with our mutagenesis data showing the crucial importance of Asp110$^{2.63}$ in binding of N/OFQ but not small molecule antagonists or the agonist SCH-221510 (Supplementary Table 5). These results suggest a similar binding mode for the "address" domains of N/OFQ-derived peptides. On the other hand, note that the κ–OR -binding peptide dynorphin A has a Pro10 in the middle of the "address" sequence[12] which is unfavorable for α-helix formation, suggesting potential differences in the binding mode for this "classical" opioid peptide.

As mentioned above, the NOP displays dramatically reduced affinities for both morphine-based small molecules and the classical OR peptide ligands: N/OFQ contains an N-terminal *F*GGF instead of the *Y*GGF motif found in the classical OR peptide ligands. Previous biochemical studies attributed this distinct selectivity profile to the three residue positions in the binding pocket of NOP that differ from all other ORs: Ala216$^{5.39}$ (Lys in others), Gln280$^{6.52}$ (His in others) and Thr305$^{7.39}$ (Ile in others). Mutation of these three positions on the N/OFQ receptor to classical OR residues has been shown to be sufficient for conferring high affinity binding to a dynorphin-derived κ–OR selective peptide[28,29]. Moreover, the same three mutations conferred nM-range NOP binding of morphine-based opioid antagonists such as bremazocine, naltrexone and naltrindole, as well as a κ–OR specific antagonist nor-BNI[29]. The crystal structures of NOP and κ–OR reveal that the side chains of these three residues are pointing towards the interior of the binding pocket (Fig. 4, Supplementary Fig. 8). In NOP, Gln280$^{6.52}$ and Thr305$^{7.39}$ are involved in C-24 interactions, while all three of the cognate residues at these positions are involved in κ–OR interactions with JDTic and with the modeled nor-BNI antagonists[1]. Interestingly, while most of the modified side chains are polar, none form direct hydrogen bonding interactions to the ligands tested, so that the selectivity profiles cannot be explained by simple polar-to-hydrophobic (or vice versa) changes of ligand contacts. Instead, a comparison of the NOP and κ–OR structures reveals that several of the NOP-specific side chain changes, including two of the substitutions mentioned above (Ala$^{5.39}$Lys, Gln$^{6.52}$His), are involved in a large-scale reshaping of the binding pocket and an alternate coordination of water molecules (Fig. 4). Located closer to the ligand binding pocket entrance, Lys227$^{5.39}$ in κ–OR, and potentially in other classical ORs, is involved in salt bridges with the side-chains of Asp223$^{5.35}$ and Glu297$^{6.58}$ (Fig. 4a). Replacement of Lys$^{5.39}$ to alanine in NOP precludes these stabilizing ionic interactions and is accompanied by an outward shift of the EC half of helix V in the NOP crystal structure, and an inward shift of helix VI. OR subtype alteration of the large Lys$^{5.39}$ side chain and the accompanying shifts of the α-helices significantly reshape the entrance to the pocket, which likely impacts the binding of "address" domains of peptides and synthetic ligands.

The κ–OR structure reveals a cluster of water molecules that is coordinated by two of the classical OR specific residues involved in binding pocket remodeling (Fig. 4b), His291$^{6.52}$ and the backbone carbonyl of Lys227$^{5.39}$. Interestingly, one such tightly bound water

Author Manuscript Author Manuscript Author Manuscript Author Manuscript

molecule is coordinated by His$^{6.52}$ and appears to preclude a buried rotamer conformation of Met$^{3.36}$ in κ–OR which is observed in NOP, resulting in a deviation of more than 6 Å between the *Cε* atoms of the side chain in these two crystal structures (Fig 4c). This Met$^{3.36}$ residue is conserved in all ORs and makes extensive hydrophobic interactions with the corresponding ligands in both NOP and κ–OR. As a consequence, the 7-hydroxyisoquinoline 'head-group' of κ–OR's ligand, JDTic, is not able to penetrate deeply into this area of the orthosteric pocket as compared with the benzofuran group of C-24. The 'reoriented' hydroxylated head-group of JDTic is stabilized by a hydrogen bond interaction to a water molecule that is coordinated by the backbone carbonyl of Lys227$^{5.39}$, potentially explaining the need for a tyrosine residue at the N-terminus of dynorphin A. With modifications of Lys$^{5.39}$ to Ala$^{5.39}$ and His$^{6.52}$ to Gln$^{6.52}$ in the NOP receptor, remodeling of the binding pocket that includes backbone shift in helix V, repacking of the Met$^{3.36}$ side chain and water rearrangements provide a likely explanation for selectivity in the "message" domain of the peptide ligands.

Perhaps most intriguing are the evolutionary differences between NOP and the other three classical opioid receptors (κ–OR, μ-OR, δ–OR). Despite high sequence identity between receptors, dramatic differences in ligand selectivity between these ORs go in hand with substantial changes in the structure of their binding pockets. This situation is very different from other GPCR subfamilies (e.g. β adrenergic, muscarinic) where different subtypes signal via the same ligands via highly conserved orthosteric pocket architectures. With structural data forκ–OR[1], μ-OR[2], and NOP now available, and the fourth (δ–OR) opioid receptor structure likely to come in the near future, one can begin to investigate the ligand structure activity relationships and evolutionary aspects of this receptor subfamily in greater detail.

Methods Summary

BRIL-NOP was expressed in *Spodoptera frugiperda* (*Sf*9) insect cells. Ligand binding asays were performed as described in Methods online. *Sf*9 membranes were solubilized using 0.5% n-dodecyl-β-D-maltopyranoside (w/v) and 0.1% cholesteryl hemisuccinate (w/v), and purified by immobilized metal ion affinity chromatography (IMAC). Receptor crystallization was performed by the lipidic cubic phase (LCP) method. The protein-LCP mixture contained 40% (w/w) concentrated receptor solution, 54% (w/w) monoolein, and 6% (w/w) cholesterol. Crystals were grown in 40 nL protein-laden LCP bolus overlaid by 0.8 μL of precipitant solution (25–30% (v/v) PEG 400, 100–200 mM potassium sodium tartrate tetrahydrate, 100 mM BIS-TRIS propane [pH 6.4]) at 20 °C. Crystals were harvested directly from LCP matrix and flash frozen in liquid nitrogen. X-ray diffraction data were collected at 100 K on the 23ID-B/D beamline (GM/CA CAT) of the Advanced Photon Source at the Argonne National Laboratory using a 10 μm collimated minibeam. Diffraction data from 23 crystals were merged for the final dataset. Data collection, processing, structure solution and refinement are described in Methods online.

Full Methods and any associated references are available in the online version of the paper at (web).

Author Manuscript Author Manuscript Author Manuscript Author Manuscript

Supplementary Material

Refer to Web version on PubMed Central for supplementary material.

Acknowledgments

This work was supported by PSI:Biology grant U54 GM094618 for biological studies and structure production, NIH Roadmap grant P50 GM073197 for technology development and R01 DA017204, R01 DA27170, and the NIMH Psychoactive Drug Screening Program (XPH, EV, BLR) and the Michael Hooker Chair of Pharmacology (BLR), University of Ferrara (FAR grant to GC), Italian Ministry of University (FIRB Futuro in Ricerca 2010 grant to CT). We thank J. Francis from Allergan for suggesting the idea to pursue the NOP receptor; J. Velasquez for help on molecular biology; T. Trinh, K. Allin and M. Chu for help on baculovirus expression; A. Walker and E. Abola for assistance with manuscript preparation; J. Smith, R. Fischetti, and N. Sanishvili for assistance in development and use of the minibeam and beamtime at GM/CA-CAT beamline 23-ID at the Advanced Photon Source, which is supported by National Cancer Institute grant Y1-CO-1020 and National Institute of General Medical Sciences grant Y1-GM-1104.

Literature Cited

1. Wu H, et al. Structure of the human kappa opioid receptor in complex with JDTic. Nature. 2012; XX:XX–XX.
2. Manglik A, et al. Crystal structure of the mu-opioid receptor bound to a morphinan antagonist. Nature. 2012; XX:XX–XX.
3. Mollereau C, et al. ORL1, a novel member of the opioid receptor family. Cloning, functional expression and localization. FEBS Lett. 1994; 341:33–38. [PubMed: 8137918]
4. Meunier JC, et al. Isolation and structure of the endogenous agonist of opioid receptor-like ORL1 receptor. Nature. 1995; 377:532–535. [PubMed: 7566152]
5. Reinscheid RK, et al. Orphanin FQ: a neuropeptide that activates an opioidlike G protein-coupled receptor. Science. 1995; 270:792–794. [PubMed: 7481766]
6. Lambert DG. The nociceptin/orphanin FQ receptor: a target with broad therapeutic potential. Nat Rev Drug Discov. 2008; 7:694–710. [PubMed: 18670432]
7. Chu R, et al. Redesign of a four-helix bundle protein by phage display coupled with proteolysis and structural characterization by NMR and X-ray crystallography. J Mol Biol. 2002; 323:253–262. [PubMed: 12381319]
8. Goto Y, et al. Identification of a novel spiropiperidine opioid receptor-like 1 antagonist class by a focused library approach featuring 3D-pharmacophore similarity. J Med Chem. 2006; 49:847–849. [PubMed: 16451050]
9. Varty GB, et al. The anxiolytic-like effects of the novel, orally active nociceptin opioid receptor agonist 8-[bis(2-methylphenyl)methyl]-3-phenyl-8-azabicyclo[3.2.1]octan-3-ol (SCH 221510). J Pharmacol Exp Ther. 2008; 326:672–682. [PubMed: 18492950]
10. Fischetti C, et al. Pharmacological characterization of the nociceptin/orphanin FQ receptor non peptide antagonist Compound 24. Eur J Pharmacol. 2009; 614:50–57. [PubMed: 19445927]
11. Volta M, Viaro R, Trapella C, Marti M, Morari M. Dopamine-nociceptin/orphanin FQ interactions in the substantia nigra reticulata of hemiparkinsonian rats: involvement of D2/D3 receptors and impact on nigro-thalamic neurons and motor activity. Exp Neurol. 2011; 228:126–137. [PubMed: 21215744]
12. Chavkin C, Goldstein A. Specific receptor for the opioid peptide dynorphin: structure--activity relationships. Proc Natl Acad Sci U S A. 1981; 78:6543–6547. [PubMed: 6118865]
13. Katritch V, Cherezov V, Stevens RC. Diversity and modularity of G protein-coupled receptor structures. Trends Pharmacol Sci. 2012; 33:17–27. [PubMed: 22032986]
14. Ballesteros JA, Weinstein H. Integrated methods for the construction of three-dimensional models and computational probing of structure-function relations in G protein-coupled receptors. Methods Neurosci. 1995; 25:366–428.
15. Wu B, et al. Structures of the CXCR4 chemokine GPCR with small-molecule and cyclicpeptide antagonists. Science. 2010; 330:1066–1071. [PubMed: 20929726]

Author Manuscript Author Manuscript Author Manuscript Author Manuscript

16. Fredriksson R, Lagerstrom MC, Lundin LG, Schioth HB. The G-protein-coupled receptors in the human genome form five main families. Phylogenetic analysis, paralogon groups, and fingerprints. Mol Pharmacol. 2003; 63:1256–1272. [PubMed: 12761335]
17. Lapalu S, et al. Comparison of the structure-activity relationships of nociceptin and dynorphin A using chimeric peptides. FEBS Lett. 1997; 417:333–336. [PubMed: 9409745]
18. Dore AS, et al. Structure of the adenosine A(2A) receptor in complex with ZM241385 and the xanthines XAC and caffeine. Structure. 2011; 19:1283–1293. [PubMed: 21885291]
19. Mouledous L, Topham CM, Moisand C, Mollereau C, Meunier JC. Functional inactivation of the nociceptin receptor by alanine substitution of glutamine 286 at the C terminus of transmembrane segment VI: evidence from a site-directed mutagenesis study of the ORL1 receptor transmembrane-binding domain. Mol Pharmacol. 2000; 57:495–502. [PubMed: 10692489]
20. Akuzawa N, Takeda S, Ishiguro M. Structural modelling and mutation analysis of a nociceptin receptor and its ligand complexes. J Biochem. 2007; 141:907–916. [PubMed: 17456499]
21. Topham CM, Mouledous L, Poda G, Maigret B, Meunier JC. Molecular modelling of the ORL1 receptor and its complex with nociceptin. Protein Eng. 1998; 11:1163–1179. [PubMed: 9930666]
22. Trapella C, et al. Structure-activity studies on the nociceptin/orphanin FQ receptor antagonist 1-benzyl-N-{3-[spiroisobenzofuran-1(3H),4′-piperidin-1-yl]propyl} pyrrolidine-2-carboxamide. Bioorg Med Chem. 2009; 17:5080–5095. [PubMed: 19527931]
23. Guerrini R, et al. Further studies on nociceptin-related peptides: discovery of a new chemical template with antagonist activity on the nociceptin receptor. J Med Chem. 2000; 43:2805–2813. [PubMed: 10956188]
24. Calo G, et al. [Nphe1,Arg14,Lys15]nociceptin-NH2, a novel potent and selective antagonist of the nociceptin/orphanin FQ receptor. Br J Pharmacol. 2002; 136:303–311. [PubMed: 12010780]
25. Tancredi T, et al. The interaction of highly helical structural mutants with the NOP receptor discloses the role of the address domain of nociceptin/orphanin FQ. Chemistry. 2005; 11:2061–2070. [PubMed: 15712334]
26. Orsini MJ, et al. The nociceptin pharmacophore site for opioid receptor binding derived from the NMR structure and bioactivity relationships. J Biol Chem. 2005; 280:8134–8142. [PubMed: 15596448]
27. Bes B, Meunier JC. Identification of a hexapeptide binding region in the nociceptin (ORL1) receptor by photo-affinity labelling with Ac-Arg-Bpa-Tyr-Arg-Trp-Arg-NH2. Biochem Biophys Res Commun. 2003; 310:992–1001. [PubMed: 14550303]
28. Meng F, et al. Moving from the orphanin FQ receptor to an opioid receptor using four point mutations. J Biol Chem. 1996; 271:32016–32020. [PubMed: 8943250]
29. Meng F, et al. Creating a functional opioid alkaloid binding site in the orphanin FQ receptor through site-directed mutagenesis. Mol Pharmacol. 1998; 53:772–777. [PubMed: 9547370]
30. Heckman KL, Pease LR. Gene splicing and mutagenesis by PCR-driven overlap extension. Nat Protoc. 2007; 2:924–932. [PubMed: 17446874]
31. Kimple AJ, et al. Structural determinants of G-protein alpha subunit selectivity by regulator of G-protein signaling 2 (RGS2). J Biol Chem. 2009; 284:19402–19411. [PubMed: 19478087]
32. Caffrey M, Cherezov V. Crystallizing membrane proteins using lipidic mesophases. Nat Protoc. 2009; 4:706–731. [PubMed: 19390528]
33. Cherezov V, Peddi A, Muthusubramaniam L, Zheng YF, Caffrey M. A robotic system for crystallizing membrane and soluble proteins in lipidic mesophases. Acta Crystallogr D. 2004; 60:1795–1807. [PubMed: 15388926]
34. Otwinowski ZMW. Processing of X-ray Diffraction Data Collected in Oscillation Mode. Methods in Enzymology. 1997; 276:19. Macromolecular Crystallography part A.
35. McCoy AJ, et al. Phaser crystallographic software. J Appl Crystallogr. 2007; 40:658–674. [PubMed: 19461840]
36. Emsley P, Lohkamp B, Scott WG, Cowtan K. Features and development of Coot. Acta Crystallogr. 2010; 66:486–501.
37. Adams PD, et al. PHENIX: a comprehensive Python-based system for macromolecular structure solution. Acta Crystallogr. 2010; 66:213–221.

Author Manuscript Author Manuscript Author Manuscript Author Manuscript

38. The PyMOL Molecular Graphics System. Version 1.4.1. Schrodinger, LLC; 2011.
39. Baker NA, Sept D, Joseph S, Holst MJ, McCammon JA. Electrostatics of nanosystems: application to microtubules and the ribosome. Proc Natl Acad Sci U S A. 2001; 98:10037–10041. [PubMed: 11517324]
40. Totrov M, Abagyan R. Flexible protein-ligand docking by global energy optimization in internal coordinates. Proteins. 1997; (Suppl 1):215–220. [PubMed: 9485515]
41. Katritch V, et al. Analysis of full and partial agonists binding to beta2-adrenergic receptor suggests a role of transmembrane helix V in agonist-specific conformational changes. J Mol Recognit. 2009; 22:307–318. [PubMed: 19353579]

Author Manuscript Author Manuscript Author Manuscript Author Manuscript

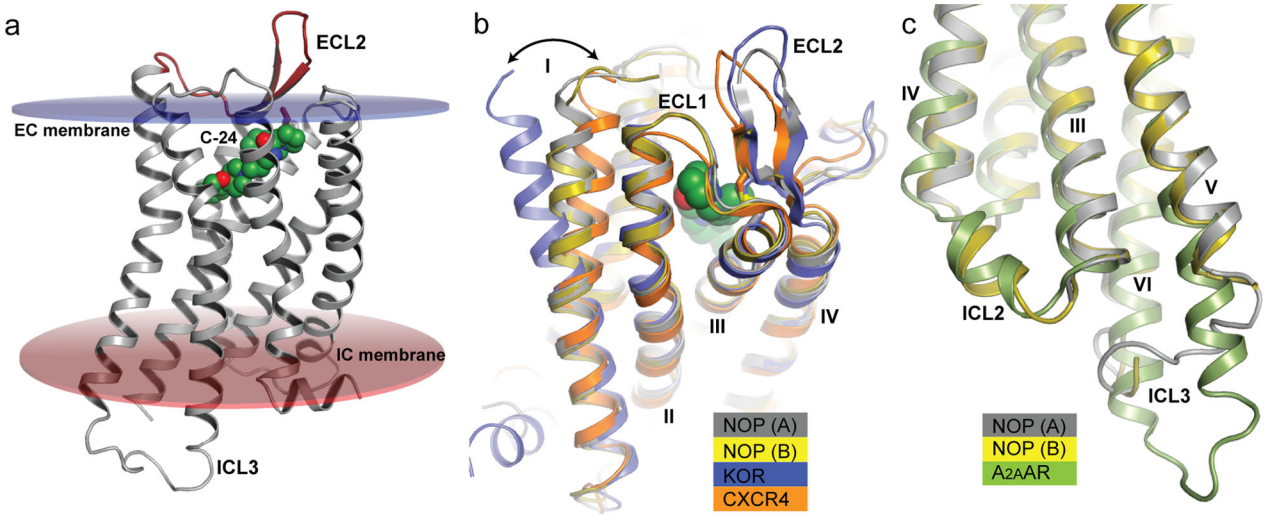

Figure 1. Structural overview of the NOP receptor

(**a**) Structural overview of NOP colored gray and ECL2 colored red. The bound ligand C-24 is depicted as green sticks, and transparent disks highlight the EC and IC membrane boundaries (colored blue and red, respectively). (**b**) Structural superposition of NOP molecules 'A' and 'B', κ–OR[1] (PDB ID 4DJH), and CXCR4[15] (PDB ID 3ODU) colored gray, yellow, blue and orange, respectively. Compared with κ–OR, the EC portion of helix I from NOP is tilted inward towards the orthosteric pocket in a conformation that is similar to CXCR4. (**c**) Structural superposition of NOP molecules 'A' and 'B' and thermostabilized $A_{2A}AR$[18] (PDB ID 3PWH) colored gray, yellow, and green, respectively, highlighting conformational differences between the ICLs.

Author Manuscript Author Manuscript Author Manuscript Author Manuscript

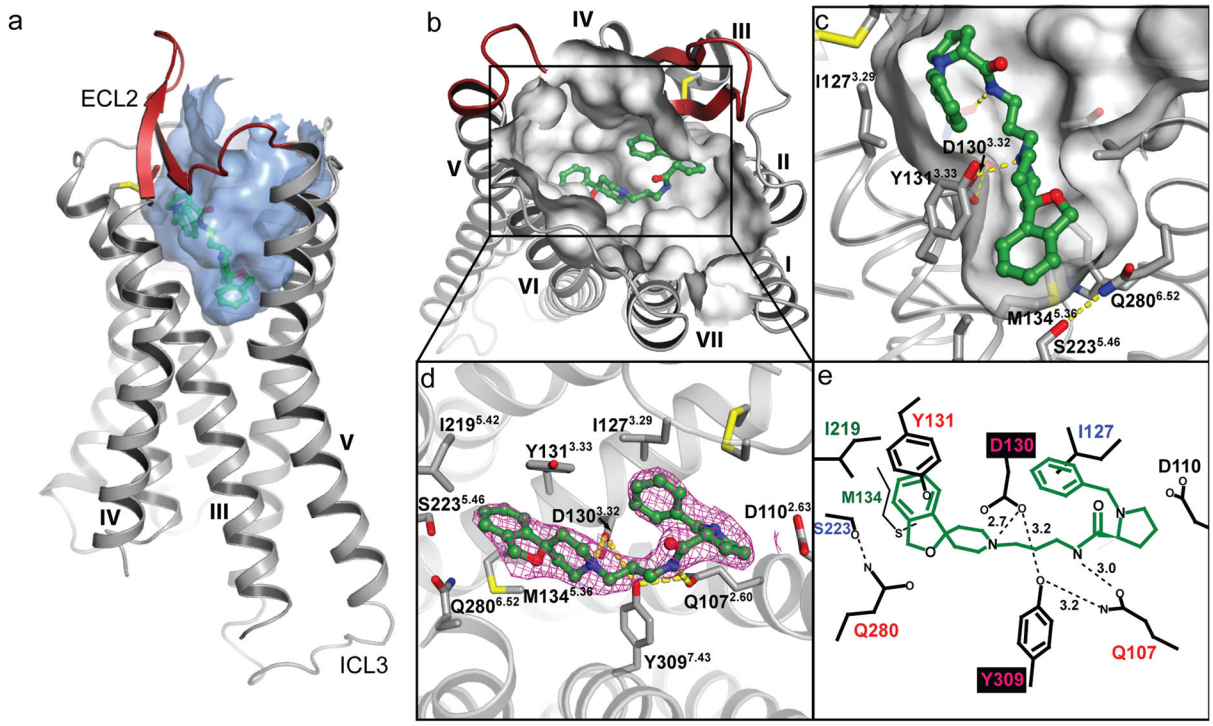

Figure 2. The orthosteric ligand binding pocket

(**a**) Cartoon representation of NOP with its large orthosteric ligand binding pocket shown as a blue transparent surface. ECL2 is colored red in all subsequent figures. (**b**) Extracellular view of the pocket with bound C-24 depicted as green sticks. (**c**) Side view of C-24 in the binding pocket with yellow dashed lines highlighting hydrogen bonding interactions and salt bridges. (**d**) Sigma-A weighted 2|mFo|-|DFc| electron density map contoured at 1.0 σ (0.0173 e/ Å ^{3}) around C-24 inside the ligand binding pocket. (**e**) Schematic representation of C-24 interactions with NOP (B) with labeled distances (Å). Residue labels are colored according to the effect on C-24 binding when replaced with alanine: Magenta labels on black background abolish C-24 binding; red labels result in ~10-fold decrease in affinity; green labeled residues slightly increase the affinity of C-24, blue labeled residues were not tested, and Asp110 had no effect on the binding of C-24, although it is crucial for N/OFQ binding.

Author Manuscript Author Manuscript Author Manuscript Author Manuscript

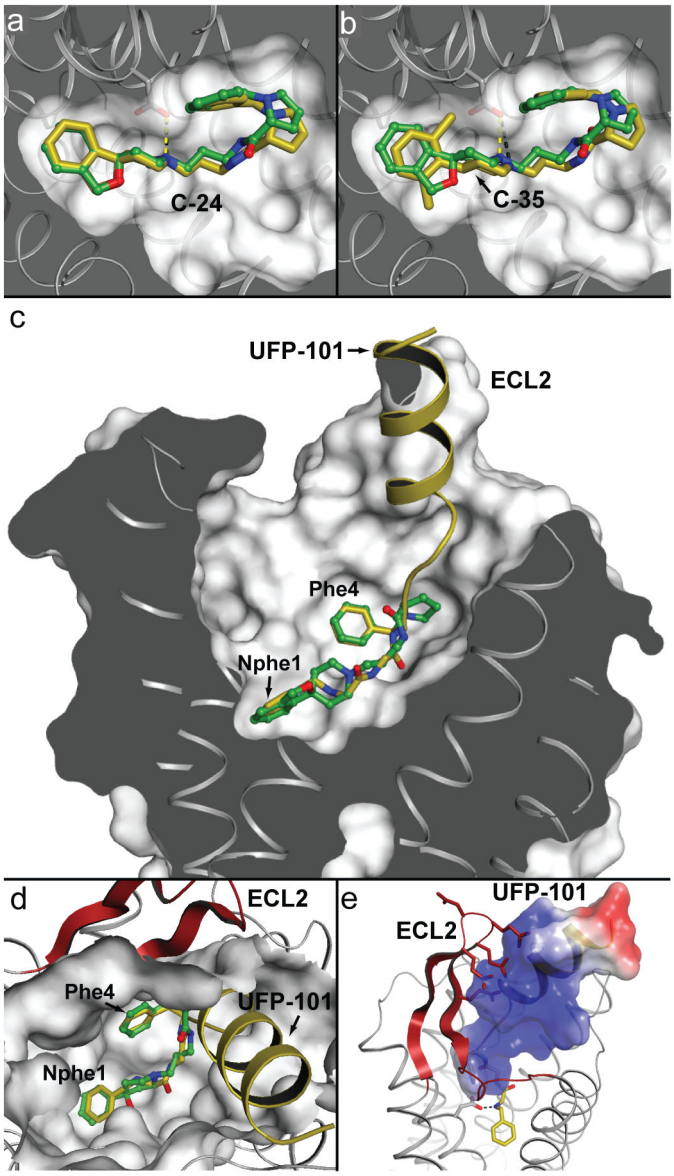

Figure 3. Molecular docking in the orthosteric binding pocket

Docking of C-24 (**a**), its analog C-35 (**b**), and peptide antagonist UFP-101 (**c, d, e**) in the NOP. The crystallographic pose of C-24 is green in all panels, and the docked molecules (C-24, C-35, UFP-101) are colored yellow. The Nphe1-Gly2-Gly3-Phe4 tetrapeptide portion of the docked UFP-101 is depicted as sticks, and the "address" domain (residues 5–17) of this peptide is represented as a cartoon. Panel (c) shows a 'sliced' side-view of the pocket; panel (d) shows a view from the extracellular surface; and panel (e) shows the electrostatic surface potentials of the UFP-101 peptide colored blue to red, corresponding to positive and negative surface potentials (+3 to −3 kT/e), respectively. ECL2 is colored red, and the acidic Asp and Glu residues from the ECL2 β-hairpin are depicted as red sticks.

Author Manuscript Author Manuscript Author Manuscript Author Manuscript

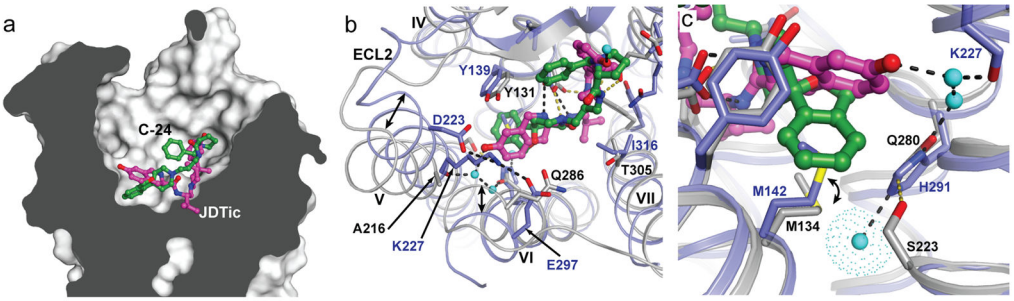

Figure 4. Conformational differences in the ligand binding pocket between NOP/C-24 and κ–OR/JDTic

(**a**) 'Sliced' surface representation of NOP highlighting the deep binding pocket bound with C-24 (colored green) and JDTic (colored magenta) from the superimposed κ–OR structure. (**b**) (**c**) Different views of NOP (colored gray with green C-24) superimposed with the κ–OR structure[1] (PDB ID 4DJH; colored blue with magenta JDTic). Hydrogen bonding interactions are depicted as dashed yellow and black lines for NOP and κ–OR, respectively. The waters from the κ–OR structure are depicted as cyan spheres. Residue labels are colored black and blue for NOP and κ–OR, respectively. Panel (a) highlights the conformational shifts observed between helices V and VI that result in differential binding pocket architectures. Panel (b) highlights the alternate rotamer of Met$^{3.36}$ (134 in NOP & 142 in κ–OR) in the pocket which affects the orientation of the ligand's head groups.